Vol. 18 No. 4 October 1, 2022 Journal of Double Star Observations

Astrometric Analysis of 4 Visual Double Star Systems

Jack Cleveland[1] and Kristen Thompson[1]

[1]Davidson College, Davidson, North Carolina

Abstract: We report astrometric observations of double stars whose physical natures were not previously known. The stars chosen for this were HJ 4034 (WDS 10202-3308), B 2842 (WDS 17425-2547), BRT 2232 (WDS 20436+3834), and SEI 897 (WDS 20075+3619). We found that BRT 2232 and SEI 897 are not physical systems, but HJ 4304 is binary and B 2842 is a likely binary candidate. For HJ 4304 and B 2842, we report on the observed separation and position angle, and use Gaia data to estimate masses and periods for both systems.

1 Overview

As the nature and future of our universe has become more well studied in the past half century, it has become increasingly apparent how important the life cycles of stars are to astrophysics, astrobiology, and cosmology. The life and death of stars dictates both how galaxies evolve and which planets and moons are capable of hosting life. It is well known that this life cycle is inherently tied to the mass of a star. To continually update evolutionary models, mass must be found independently of other factors that evolve over time, such as luminosity. This is impossible for single stars, but binary stars can have their masses determined by finding their orbital elements. Finding and studying these stars will add to the knowledge of the dynamic process of stellar evolution and inform further research.

In this paper, we present new astrometric measurements of four double star pairs and the determinations made about whether they are true binaries or optical doubles. These subjects were visual doubles selected from the Washington Double Star (WDS) catalog (Mason et al., 2015) whose nature was not previously known. Our measurements, alongside information provided by the Gaia Data Releases 2 (DR2) and 3 (DR3) (Gaia Collaboration 2016, 2018, 2022 (in prep)), have been used to make estimations of mass and the period where possible.

The theory used in this analysis is described in Section 2, technical methods are presented in Section 3, and results are discussed in Section 4. Our conclusions are given in Section 5.

Received Date

2 Theory

For stars in a binary system, the separation (ρ) and position angle (θ) are expected to change over time. For each target source, these values were measured and their change over time visualized in the Plot Tool 3.1 from Harshaw (2020). In addition, the Plot Tool was used to calculate the average physical separation, weighted by the uncertainty in parallax, between the stars in the system.

Additional information about the stars was gathered from the Gaia DR2 and DR3 catalogs. Gaia DR3 parallax information was used to calculate the distance to the systems using the parallax formula

$$d = \frac{1}{p}, \tag{1}$$

where the distance (d) is measured in parsecs and the parallax (p) in arcseconds. Gaia DR3 apparent G-band magnitudes (m) and Gaia DR2 G-band extinction measurements (A) were used in combination with the calculated distance to the system to determine absolute magnitudes (M_A) of the stars via the distance modulus

$$M_A + A = m - 5log\left(\frac{d}{10}\right). \tag{2}$$

Once the absolute magnitude of a star was found, it was used to find the luminosity (L) of that star using the relation

$$M_{A\odot} - M_A = 2.5log\left(\frac{L}{L_\odot}\right), \tag{3}$$

where the subscript $\odot$ refers to properties of the Sun as a reference star. Luminosity was then used to calculate stellar mass using the mass luminosity equation for main sequence stars

$$\frac{L}{L_\odot} = \left(\frac{M}{M_\odot}\right)^4, \tag{4}$$

where M and $M_\odot$ are the mass of the observed star and the Sun, respectively.

As described by Halbwachs (1986), sub-giant stars are on average one magnitude brighter than they would be if they were main sequence stars. Main sequence relationships can be used to determine sub-giant properties if the observed sub-giant apparent magnitude m is replaced with $m+1$. Therefore, sub-giant luminosities and masses were determined by making this apparent magnitude substitution into Equation 2 and applying Equations 3 and 4.

These masses, alongside weighted physical separations determined from the Plot Tool, can be used to calculate period using Kepler's third law

$$M_1 + M_2 = \frac{4\pi^2}{G}\frac{1}{P^2}\left(\frac{a}{cos(i)}\right)^3, \tag{5}$$

where M_1 and M_2 are the primary and secondary stellar masses, a is the semi-major axis, G is the gravitational constant, i is inclination, and P is period. This equation assumes the physical separation is a rough equivalent to the semi-major axis, and takes an average value for $(cos(i))^3$ to be 0.424 from Carroll and Ostlie (2017).

3 Methods

The Stelle Doppie Double Star Database (Sordiglioni, 2020) and the Gaia Double Star (GDS) Selection Tool (Rowe, 2020) were used to create a list of candidate systems. Right ascension (α) was limited to 7^h to 23^h to exclude stars that were not visible between our observation dates of 26 May 2022 and 22 June 2022. Declination (δ) was allowed to range between -80° and +80°. Apparent magnitude was set between 7 and 11 and magnitude difference (Δm) was limited to 3 to ensure independently visible targets that can be observed with reasonable exposure times. Separation had a minimum value $5''$ to match the resolving power of the imaging system. Sources chosen for further study, and their characteristic properties taken from Stelle Doppie, are given in Table 1.

The 0.4 m telescopes of the Las Cumbres Observatory global telescope (LCOGT) network were used in combination with the attached SBIG STL6303 CCD cameras to image each target source. The PANSTARRS-w filter was chosen for maximum coverage of the visible spectrum in the images, and the exposure time was chosen for each source according to the magnitudes of the primary and secondary components of the pair.

Prior to conducting a full set of observations, brief test observations were conducted to ensure proper exposure times and quickly check that astrometric data could be gathered for each source. These test observations revealed that the relative positions of stars in SEI 987 and BRT 2232 did not match what was expected given WDS and Stelle Doppie catalog data. Therefore, full measurements of separation and position angle for these two sources were not taken. A discussion of the test observations and some properties of these sources revealed by the test images and catalog data can be found in Sections 4.3 and 4.4. Following careful inspection of the test observations, 15 additional images were taken of target sources HJ 4304 and B 2842 for full astrometric analysis.

Initial data calibration was automatically performed by the LCOGT pipeline (Fitzgerald, 2018) prior to download. Once downloaded, the images were imported into AstroImageJ (Collins et al., 2017). The Aladin Sky Atlas (Bonnarel et al., 2000) served as a cross-reference for the star field in each image and was used to confirm the targets were present. The aperture photometery tool in AstroImageJ with the Howell centroiding method (Howell, 2006) was used to measure values for separation and position angle in each image. Both HJ 4304 and B 2842 used sky annulus settings of 35 pixels for the inner ring, 40 pixels for the outer ring, and 6 pixels for the inner aperture radius. Measurements of ρ and θ for each source, as well as average values for both measurements, are given in Section 4.

4 Analysis and Results

WDS historical data was requested from and provided by Dr. Brian Mason of the United States Naval Observatory (USNO). This was imported into the Plot Tool 3.19 to construct graphs of the position of the secondary star relative to the primary over time. Individual source analysis details can be found in Subsections 4.1 - 4.4.

4.1 HJ 4304

HJ 4304 (WDS 10202-3308) was discovered in 1836 by John Hershel. This is the brightest system in this study, as the primary star is 2 magnitudes brighter than other chosen targets. A full set of 15 observations was carried at the Cerro Tololo Inter-American Observatory on 7 June 2022 with an exposure time of 1 second. A sample image from these observations is shown in Figure 1, annotated with measured values of separation and position angle. Measurements of these quantities for all images can be be found in Table 2.

Table 1: Characteristics of Target sources

	HJ 4304	B 2842	SEI 987	BRT 2232
α (J2000)	$10^h\ 20^m\ 13.67^s$	$17^h\ 42^m\ 28.60^s$	$20^h\ 07^m\ 36.78^s$	$20^h\ 43^m\ 32.66^s$
δ (J2000)	-33° 07′ 43.4″	-25° 45′ 39.5″	20° 19′ 33.2″	38° 33′ 15.5″
Discovered	1836	1911	1896	1928
Primary Mag	7.55	9.53	10.92	10.48
Δm	2.23	1.98	0.98	1.72
Last Obs ρ	9.5″	9.2″	18.2″	5.8″
Last Obs θ	287°	269°	286°	345°
Last Obs Year	2016	2015	2010	2003

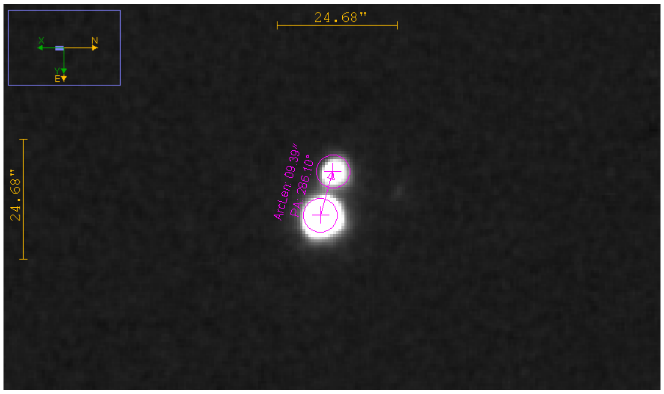

Figure 1: Analysis of image 11 of HJ 4304 as seen in AstroImageJ. These measurements of separation and position angle were averaged with the values from the rest of the images to determine the final values. For this image, the separation and position angle were measured to be 9.39″ and 286.10°, respectively.

Table 2: Sampled Data for HJ 4304

Observation	ρ(″)	θ(°)
1	9.42	286.03
2	9.47	286.11
3	9.28	286.43
4	9.41	285.79
5	9.47	285.87
6	9.39	285.97
7	9.39	285.77
8	9.44	285.88
9	9.39	286.21
10	9.35	286.13
11	9.39	286.10
12	9.32	286.20
13	9.39	285.88
14	9.31	285.95
15	9.28	286.49
Average	9.38	286.05
Standard Deviation	0.06	0.22
Standard Error of Mean	0.02	0.06

Table 3: Historical Data for HJ 4304

Year	ρ (″)	θ(°)	Reference
1836.13	12.	289.7	Herschel (1847)
1898.34	9.70	286.7	See (1927)
1911.30	9.872	288.0	Urban et al. (1998)
1914.38	10.300	285.2	Urban et al. (1998)
1920.06	9.59	285.9	Tapia (1921)
1920.08	9.60	286.0	Dawson (1922)
1928.34	9.48	288.6	van den Bos et al. (1964)
1934.01	9.30	285.9	Wallenquist (1938)
1991.25	9.451	286.5	ESA (1997)
1991.46	9.45	286.5	Fabricius et al. (2002)
1999.122	9.430	286.1	Hartkopf et al. (2013)
1999.22	9.37	286.4	2MASS Catalog (2003)
2004.37	9.488	286.40	Sinachopoulos et al. (2007)
2015.0	9.463	286.434	Knapp and Nanson (2019)
2015.5	9.46303	286.433	El-Badry and Rix (2019)
2016.0	9.46326	286.43	El-Badry et al. (2021)

Historical data for HJ 4304 is provided in Table 3. Measurements are given to the precision provided by the referenced sources, shown in the last column. Observations made between 1835 and 1934 were found to have significant variability, with a range of values for ρ and θ that vary by 0.7″ and 3.4°, respectively, over the approximately 99 years of observation. This is an order of magnitude greater than the range of values for observations made after 1990 of 0.08″ and 0.45° for ρ and θ, respectively. Because the modern values were more consistent, we excluded data prior to 1934 from our analysis. The uncertainty in the earlier data is likely generated from the technical limitations of the time period, making this data unfit for analysis.

Figure 2 shows the relative position of the secondary in regards to the primary, located at the origin. Each data point represents an observation made at a time. In this figure, historical observations are shown in blue and the result of the current study in red. Note that some measurements have nearly identical values for ρ and θ and therefore overlap in the plot. The observation being reported in this study appears lowest along the y-axis, while the earliest entry appears highest on the y-axis, suggesting the secondary may be travelling along a line between them. However, no other points appear in chronological order. The large scatter suggests the real values of ρ and θ have changed little over time and the differences are occluded by uncertainty. This data is insufficient to be used as part of an orbital approximation.

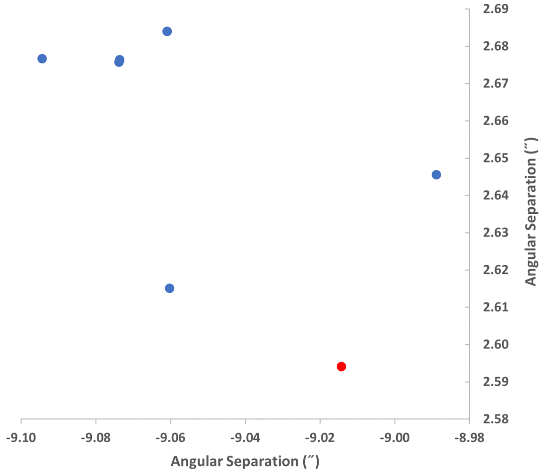

Figure 2: Relative motion of HJ 4304 produced by Plot Tool 3.19. The data presented in this study appears in red. Historical data appears in blue. North is in the positive direction of the Y-axis, while east is in the positive direction of the X-axis.

Table 4 shows the values for parallax, its uncertainty, and the proper motion in both right ascension (PMRA) and declination (PMD) for HJ 4304 taken from Gaia DR3. The distance to the primary and secondary components, found using DR3 parallax and Equation 1, was 123.91 pc and 123.29 pc, respectively.

Combining these calculated distances with the observed average separation, the two stars have a weighted physical separation of 1159 AU. Given the small uncertainty in parallax, the nearly identical stellar distances, and the calculated separation, it is reasonable to conclude that the system may be physically related. Furthermore, proper motion indicates the primary and secondary are traveling together, which also supports a gravitationally bound binary system.

Table 4: Gaia Data for the HJ 4304 System.

	HJ 4304 A	HJ 4304 B
Parallax (mas)	8.0703	8.1107
Parallax Error (mas)	0.0274	0.0169
PMRA (mas yr^{-1})	-24.235	-24.630
PMD (mas yr^{-1})	11.235	11.038
G-mag	7.52	9.74

While an orbital model cannot be made, the method described in Section 2 can be used to calculate masses. The primary star of HJ 4304 is listed as a sub-giant in Stelle Doppie, and as such we used the modified version of Equation 2 for the determination of absolute magnitude. The masses were calculated to be $1.64M_{\odot}$ for the primary and $1.14M_{\odot}$ for the secondary. These masses alongside the physical separation yield a period of 36,374 years using Equation 5. This is a reasonable period for a binary pair of this physical separation. The total time span of observations was less than 1 percent of the total period, making orbital calculation difficult, especially with the variability in historical data.

These results lead us to conclude that HJ 4304 is a true binary system. The estimates of mass and period, along with proper motion and parallax, suggest a binary system with a separation slightly larger than average. The system currently lacks enough data to display an orbital trend, and it will take significantly more data for an orbital solution to be resolved. Observations in the near future can help refine the mass and period estimates until sufficient data has been collected to allow for a calculation of a model.

4.2 B 2842

B 2842 (WDS 17425-2547) was discovered by Willem Hendrik van den Bos in 1911. A full set of 15 images of this source was carried out on 22 June 2022 at Siding Spring Observatory with a 1 second exposure time.

Measurements of separation and position angle from AstroImageJ can be seen in Table 5. The average separation and position angle were found to 9.196″ and 344.86°, respectively. Historical data for this source can be found in Table 6. Entries are given to the precision of the referenced sources, shown in the last column. Observations from 1911.5, 1930, and 1999.51 were omitted from this study because the measurements of separation and position angle did not agree well with other measurements. The new measurements from this study are consistent with other recent observations from the historical data. A sample image and measurement of ρ and θ for this source can be found in Figure 3.

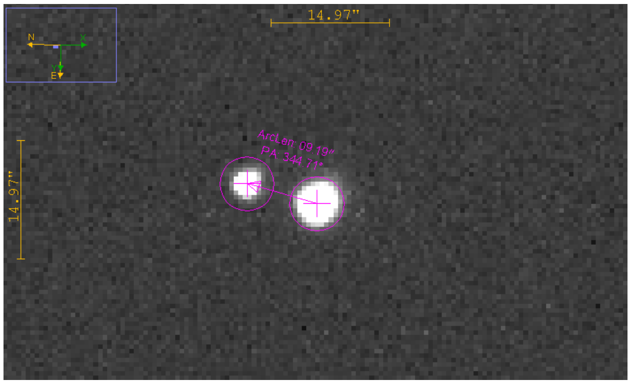

Figure 3: Analysis of image 6 of B 2842 as seen in AstroImageJ. These measurements of separation and position angle were averaged with the values from the rest of the images to determine the final values. For this image, the separation and position angle were measured to be 9.19″ and 344.71°, respectively.

Table 5: Sampled Data for B 2842

Observation	$\rho('')$	$\theta(^\circ)$
1	9.24	344.89
2	9.19	344.64
3	9.19	344.64
4	9.17	344.88
5	9.20	344.66
6	9.19	344.71
7	9.15	345.11
9	9.24	344.65
10	9.20	344.72
11	9.19	345.11
12	9.20	345.09
13	9.23	344.77
15	9.17	345.27
Average	9.196	344.86
Standard Deviation	0.026	0.2099
Standard Error of Mean	0.007	0.0582

Table 6: Historical Data for B 2842

Year	$\theta(^\circ)$	$\rho('')$	Reference
1911.5	347.4	9.811	Urban et al. (1998)
1913.44	343.9	9.780	Urban et al. (1998)
1930.0	315.0	8.0	van den Bos (1930)
1964.68	345.5	9.12	van den Bos (1968)
1987.353	344.9	9.18	Sinachopoulos (1988)
1999.384	344.8	9.134	Hartkopf et al. (2013)
1999.51	342.2	8.92	2MASS Catalog (2003)
2015.0	344.606	9.210	El-Badry and Rix (2019)
2015.5	344.602	9.169	Knapp and Nanson (2019)

The historical data looks to display a trend initially. All observations show a decreasing value for the position angle, excluding the one from the year 1964.68. The change in position angle between adjacent observations appears to be decreasing at a decelerating rate. The orbital speed of a binary pair varies as the distance between the stars changes. If the pair is physically related, this change in position angle could be caused by the secondary slowing down in its orbit as it approaches apogee or the uncertainty of the measurements getting increasingly smaller with time. As seen in Table 6, the separation between the stars is generally linearly increasing although, unlike for position angle, there is no smooth trend. This could correspond with the secondary approaching apogee, but with uncertainty in the historical data, it is not possible to confirm.

To further explore the motion of the secondary with respect to the primary component, the average rate of change for both ρ and θ were determined. To find the average rate of change, we took the difference in both ρ and θ between adjacent observations and then divided by the number of years between observations. Figure 4 shows the average rate of change in position angle, with the x-axis values being the average date between observations. Both the position angle and the rate at which it is changing are generally decreasing over time. The change in separation per year can be seen in Figure 5. It is interesting to note that the rate of change in separation is nearly zero for all intervals such that the separation is nearly constant with time. However, no clear conclusion about the nature of the stars can be drawn from these graphs due to small sample size and variability in the historical data.

The relative motion of the secondary of B 2842 about the primary is shown in Figure 6. Historical data appear in blue, while the value from the current study appears in red. Since the newest entry is in the middle of a collection of points, a discernible track cannot be found.

Gaia DR3 data (see Table 7) was used to learn more about the pair in the absence of an orbital solution. Parallax data is similar with both stars having parallaxes of approximately 8.6 mas. Using the individual parallaxes, the primary and secondary stars are found to have distances of 116.2 pc and 116.3 pc, respectively. If uncertainty in parallax is considered in distance calculations, the range of distances to both stars are found to overlap by 80 percent. The weighted physical separation between the stars was found to be 1070 AU. This is comparable to the average separation of 800 AU for all confirmed binaries in the Sixth Orbital Catalog (Harshaw, 2020; Matson et al., 2022). The difference in proper motions

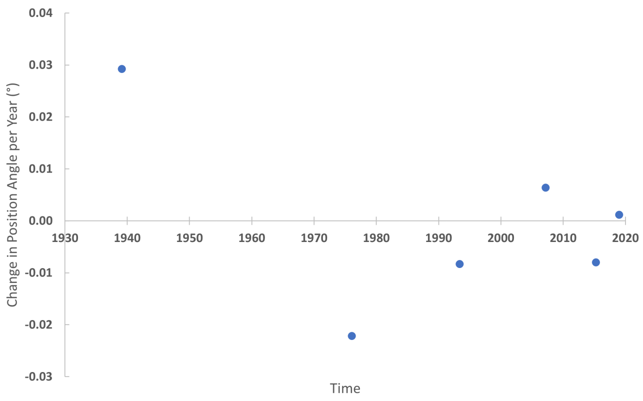

Figure 4: The rate of change in position angle per year for B 2842. This was calculated by taking the difference between the position angle recorded in two consecutive observations, and then dividing by the number of years between those observations. The x-axis values are the average year between observations.

for the two stars is 1.346 mas yr^{-1} for right ascension and 0.247 mas yr^{-1} for declination. While the common distances and close physical separation of the pair is supportive of a binary system, the proper motions are not as similar. Therefore, while this system may indeed be physically related, further study is necessary to draw strong conclusions.

	B 2842 A	B 2842 B
Parallax (mas)	8.6033	8.5981
Parallax Error (mas)	0.0251	0.0313
PMRA (mas yr^{-1})	11.007	9.654
PMD (mas yr^{-1})	24.493	24.754
G-mag	9.33	11.21

Table 7: Gaia Data for the B 2842 System

Given the small physical separation of the system and the possibility that it is gravitationally bound, we use methods from Section 2 to determine possible masses and an orbital period for the system. We found masses for the primary and secondary of $1.27M_{\odot}$ and $0.80M_{\odot}$, respectively, and a period of 37,394 years.

It is possible B 2842 is a true binary pair. The physical separation is close enough for the system to be gravitationally bound, but proper motion does not strongly confirm this. The orbital period is typical but, with too little data to create an orbital model, we cannot confirm the pair is a true binary. Additional observations will be needed to allow for the determination of an orbit.

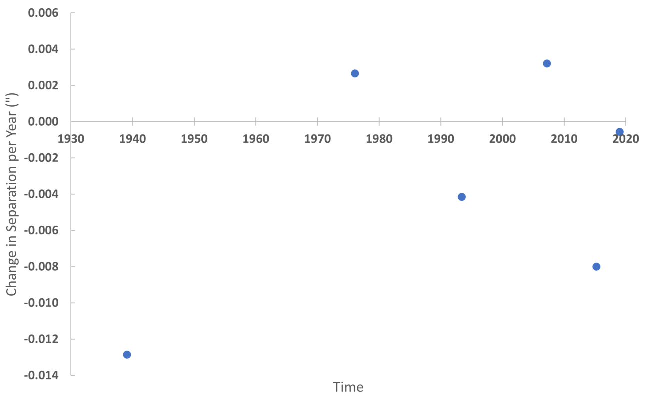

Figure 5: The rate of change in separation per year for B 2842. This was calculated by taking the difference between the separation recorded in two consecutive observations, and then dividing by the number of years between those observations. The x-axis values are the average year between observations.

4.3 BRT 2232

BRT 2232 (WDS 20436+3834) was discovered by S. G. Barton in 1928. This pair had not been observed since 2004, and according to Stelle Doppie has a variable position angle. Two test observations were conducted at Teide Observatory on 27 May 2022, with 3 seconds of exposure per image, and 7 June 2022, with 1.75 seconds of exposure per image.

We decided to eliminate BRT 2232 from contention for full observation due to the appearance of test images. One of the test measurements can be found in Figure 7. The position angle measured was approximately 90°, almost exactly 180° different than the expected value of 270° from Stelle Doppie. A second test was scheduled to see if the difference was the result of a problem with the observation. The Teidi Observatory 0.4 meter telescope of the LCOGT was used for both observations, and the same position angle was observed in both images. We were unable to explain such a discrepancy and as such abandoned the candidate for full observation.

Further investigation of the source using data from Gaia DR3 revealed distances to each star that were significantly different. Parallax and proper motion data for BRT 2232 can be seen in Table 8. Using Equation 1, distances to the primary and secondary were determined to be 769 pc and 315 pc, respectively. These distances, along with the value for ρ from Stelle Doppie, were used with the law of cosines to find a physical separation. This resulted in a separation of 453 pc, much too great to be physically related. Proper motion additionally indicates the two are traveling in different directions. Both physical separation and proper motion leads us to con-

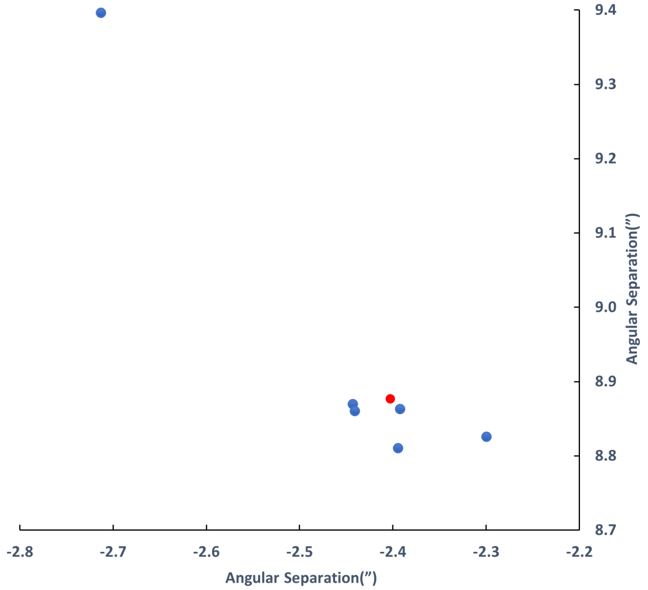

Figure 6: The relative motion of B 2842 produced by Plot Tool 3.19. The data presented in this study appears in red. Historical data appears in blue. North is in the positive direction of the Y-axis, while east is in the positive direction of the X-axis.

clude that this is an optical double.

The sudden change in position angle seen in test images cannot be explained by the non-physical nature of BRT 2232. The proper motions of BRT 2232 are too slow for the secondary to have passed behind and to the other side of the primary considering the twenty-year gap in observations. We suspect it may be an artifact of observation rather than a true shift in stellar positions. Independent measurements of position angle taken from the Teide Observatory for target source SEI 897, observed within an hour of the first test observation of BRT 2232, produced expected position angles. We therefore believe the difference in position angle to not be a result of telescopic error. Future investigation into the observed position angle could further characterize the nature of this apparent shift.

	BRT 2232 A	BRT 2232 B
Parallax (mas)	1.3012	3.1738
Parallax Error (mas)	0.0130	0.0158
PMRA (mas yr^{-1})	-10.508	8.418
PMD (mas yr^{-1})	-10.929	-3.921

Table 8: Gaia Data for the BRT 2232 System

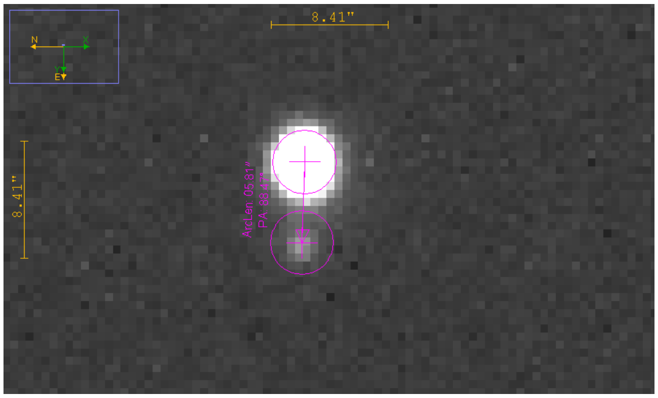

Figure 7: Analysis of a test image of BRT 2232 as seen in AstroImageJ. Due to the unexpected relative positions of the primary and secondary stars, BRT 2232 did not receive a full set of observations.

4.4 SEI 897

SEI 897 (WDS 20075+3619) was discovered in 1896 by Julius Scheiner, and had not been observed since 2010. The pair has a separation of about 18″ compared to under 10″ for the rest of the targets in this study. Two test observations were preformed at the Teide Observatory on 26 May 2022 with an exposure time of 2.5 seconds and on 27 May 2022 with an exposure time of 1 second.

Full observations for SEI 897 were not scheduled because of difficulty identifying the secondary star in test images. Stelle Doppie reports expected values for ρ and θ of 18.2″ and 287°, respectively. As seen in Figure 8, there were several stars near the primary. The red X in the image indicates the position of the secondary as indicated by Stelle Doppie. One star, under the cross-hair in the image, was found near to the expected position. However, the Δm between this source and the primary was 4.0 magnitudes, not in agreement with the Δm of 0.98 magnitudes reported by Stelle Doppie.

Unable to confidently identify the secondary star, we decided to investigate other nearby stars. Using the online tool VizieR (Kharchenko et al., 2012), we found Gaia DR2 data for every star within 36″ of the primary. One star with approximately the expected separation and position angle was found. The Δm between this star and the primary of SEI 897 was approximately 4.0 magnitudes, matching was was observed in the test image, but not what was expected given Stelle Doppie data. We believe this star to be the one that was measured in the test data, and shown in Figure 8.

With the Δm reported in Stelle Doppie so dissimilar to observations, the possibility that SEI 897 B was a variable star was considered. The Variable Star Index (VSX) (Mason et al.,

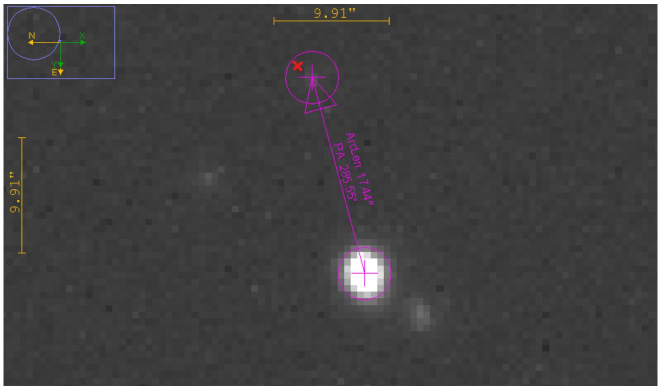

Figure 8: Analysis of a test image of SEI 897 as seen in AstroImageJ. For this image, the separation and position angle were measured to be 17.44″ and 285.55°, respectively. Due to difficulty identifying the secondary star, SEI 897 did not receive a full set of observations.

2015) does indeed list the star identified as the secondary as a variable star. However, the VSX reports the Sloan r-band variability to be 0.181 magnitudes. While Gaia and Stelle Doppie report G-band magnitudes, the variability reported by VSX is unlikely to resolve the observed Δm of nearly 3 magnitudes larger than expected. Due to this inconsistency in magnitude and the uncertainty in the identification of the secondary star, we did not conduct further observations of source.

As with BRT 2232, Gaia DR3 was used to determine the physical nature of SEI 897. Parallax, proper motion in both right ascension and declination, and G-band magnitudes for the primary and the star suspected to be the secondary can be found in Table 9. The proper motion of the pair indicates the primary and secondary are generally traveling in the same direction. Distances to each star were calculated with Equation 1. These masses and the ρ value taken from Stelle Doppie were used to compute the physical separation with the law of cosines, which was found to be 3961 pc. This physical separation is much too large for these stars to be gravitationally bound. If further observations of this optical double are desired, the variability in magnitude must be resolved.

	SEI 897 A	SEI 897 B
Parallax (mas)	3.2089	0.2340
Parallax Error (mas)	0.0273	0.0164
PMRA (mas yr^{-1})	-17.663	-2.406
PMD (mas yr^{-1})	-14.021	-3.041
G-mag	10.76	14.35

Table 9: Gaia data for the SEI 897 System

5 Conclusions

HJ 4304 was found to be a binary and B 2842 was found to be a likely binary candidate. While full orbital solutions were unable to be calculated for these sources, period estimates were calculated with Kepler's third law. More observations in the near future for these pairs should continue to update the period and mass estimates, and provide historical data points that can be used to create a well-fitting orbital model. BRT 2232 and SEI 897 were found to be optical doubles. While neither is a binary star, both have observed characteristics that would be interesting to further investigate. Additional observations over a longer fraction of the orbit for the binary pairs, and more information to resolve conflicts in expected positions and magnitudes for the optical doubles, are needed to fully characterize these targets.

Acknowledgments

This work has made use of data from the European Space Agency (ESA) mission Gaia (`https://www.cosmos.esa.int/gaia`), processed by the Gaia Data Processing and Analysis Consortium (DPAC, `https://www.cosmos.esa.int/web/gaia/dpac/consortium`). Funding for the DPAC has been provided by national institutions, in particular the institutions participating in the Gaia Multilateral Agreement.

This research has made use of the Washington Double Star Catalog maintained at the U.S. Naval Observatory.

This work has made use of observations from the Las Cumbres Observatory

This research has made use of data from the Stelle Doppie double star catalog.

This research has made use of the Gaia Double Star Selection tool.

This research has made use of the VizieR catalogue access tool, CDS, Strasbourg, France.

This research has made use of the International Variable Star Index (VSX) database, operated at AAVSO, Cambridge, Massachusetts, USA.

References

2MASS Catalog, R. (2003). 2mass point src cat. all-sky release.

Bonnarel, F., Fernique, P., Bienaymé, O., Egret, D., Genova, F., Louys, M., Ochsenbein, F., Wenger, M., and Bartlett, J. G. (2000). The ALADIN interactive sky atlas. A reference tool for identification of astronomical sources. A&AS, 143:33–40.

Carroll, B. W. and Ostlie, D. A. (2017). *An introduction to modern astrophysics*. Cambridge University Press.

Collins, K. A., Kielkopf, J. F., Stassun, K. G., and Hessman, F. V. (2017). AstroImageJ: Image Processing and Photometric Extraction for Ultra-precise Astronomical Light Curves. AJ, 153(2):77.

Dawson, B. H. (1922). Resultado de las observaciones con la ecuatorial de 433 milimetros de abertura : effectuadas de 1918.0 a 1921.5. *Observatory Astronomical La Plata Series Astronomies*, 4:iv.

El-Badry, K. and Rix, H.-W. (2019). The wide binary fraction of solar-type stars: emergence of metallicity dependence at a ¡ 200 au. MNRAS, 482(1):L139–L144.

El-Badry, K., Rix, H.-W., and Heintz, T. M. (2021). A million binaries from Gaia eDR3: sample selection and validation of Gaia parallax uncertainties. MNRAS, 506(2):2269–2295.

ESA (1997). VizieR Online Data Catalog: The Hipparcos and Tycho Catalogues (ESA 1997). *VizieR Online Data Catalog*, page I/239.

Fabricius, C., Høg, E., Makarov, V., Mason, B., Wycoff, G., and Urban, S. (2002). The tycho double star catalogue. *Astronomy & Astrophysics*, 384(1):180–189.

Fitzgerald, M. T. (2018). The Our Solar Siblings Pipeline: Tackling the data issues of the scaling problem for robotic telescope based astronomy education projects. *Robotic Telescope, Student Research and Education Proceedings*, 1(1):347–358.

Gaia Collaboration (2016). The Gaia mission. A&A, 595:A1.

Gaia Collaboration (2018). Gaia Data Release 2. Summary of the contents and survey properties. A&A, 616:A1.

Gaia Collaboration (2022, in prep). Gaia DR3: data release content and main properties. A&A.

Halbwachs, J. L. (1986). Binaries among bright stars: systems with evolved primary components and their relation to the properties of main-sequence binaries. A&A, 168:161–168.

Harshaw, R. (2020). Using plot tool 3.19 to generate graphical representations of the historical measurement data. *Journal of Double Star Observations*, 16(4):386–400.

Hartkopf, W. I., Mason, B. D., Finch, C. T., Zacharias, N., Wycoff, G. L., and Hsu, D. (2013). Double stars in the usno ccd astrographic catalog. *The Astronomical Journal*, 146(4):76.

Herschel, John Frederick William, S. (1847). *Results of astronomical observations made during the years 1834, 5, 6, 7, 8, at the Cape of Good Hope; being the completion of a telescopic survey of the whole surface of the visible heavens, commenced in 1825*.

Howell, S. B. (2006). *Handbook of CCD Astronomy*, volume 5.

Kharchenko, N. V., Piskunov, A. E., Roeser, S., Schilbach, E., and Scholz, R. D. (2012). VizieR Online Data Catalog: Milky Way global survey of star clusters (Kharchenko+, 2012). *VizieR Online Data Catalog*, pages J/A+A/543/A156.

Knapp, W. and Nanson, J. (2019). A Catalog of High Proper Motion Stars in the Northern Sky (HPMSNS Catalog). *Journal of Double Star Observations*, 15(1):42–58.

Mason, B. D., Wycoff, G. L., Hartkopf, W. I., Douglass, G. G., and Worley, C. E. (2015). VizieR Online Data Catalog: The Washington Visual Double Star Catalog (Mason+ 2001-2014). *VizieR Online Data Catalog*, page B/wds.

Matson, R. A., Williams, J., S., Hartkopf, W. I., and Mason, B. D. (2022). Sixth catalog of orbits of visual binary stars. `http://www.astro.gsu.edu/wds/orb6.html`. Accessed: 26 July 2022.

Rowe, D. (2020). Gaia Double Star Selection Tool. 1.02.

See, T. (1927). Southern double star catalog.

Sinachopoulos, D. (1988). CCD measurements of visual binaries. A&AS, 76:189–193.

Sinachopoulos, D., Gavras, P., Dionatos, O., Ducourant, C., and Medupe, T. (2007). Ccd astrometry and components instrumental magnitude difference of 432 hipparcos wide visual double stars. *Astronomy & Astrophysics*, 472(3):1055–1057.

Sordiglioni, G. (2020). Stelle Doppie Double Star Database. 2.7.1.

Tapia, N. (1921). Medidas micrometricas de estrellas dobles Y vecinas. *Observatory Astronomical La Plata Series Astronomies*, 6:16–41.

Urban, S., Corbin, T., Wycoff, G., Martin, J., Jackson, E., Zacharias, M., and Hall, D. (1998). The ac 2000: The astrographic catalogue on the system defined by the hipparcos catalogue. *The Astronomical Journal*, 115(3):1212.

van den Bos, W. H. (1930). New southern double stars, tenth list. Bull. Astron. Inst. Netherlands, 5:179.

van den Bos, W. H. (1968). Micrometer Measures of Double Stars. *Republic Observatory Johannesburg Circular*, 127:157–161.

van den Bos, W. H., Donner, H. F., and Jessup, M. K. (1964). Micrometer measurements of southern double stars, made with the 27-inch refractor of the Lamont-Hussey Observatory. *Publications of Michigan Observatory*, 9(4):73–111.

Wallenquist, Å. (1938). Photographic and Photovisual Magnitudes for some Supplementary Polar Stars. In *Professor Östen Bergstrand Vetenskapsmannen Och Läraren*, page 39.